Association of lithocholic acid with skeletal muscle hypertrophy through TGR5-IGF-1 and skeletal muscle mass in chronic liver disease rats and humans.

Yasuyuki Tamai[1#], Akiko Eguchi[1#], Ryuta Shigefuku[1], Hiroshi Kitamura[2], Mina Tempaku[1], Ryosuke Sugimoto[1], Yoshinao Kobayashi[3], Motoh Iwasa[1], Yoshiyuki Takei[1] and Hayato Nakagawa[1]

[1]Department of Gastroenterology and Hepatology, Mie University Graduate School of Medicine, [2]Department of Veterinary Medicine, School of Veterinary Medicine, Rakuno Gakuen University, [3]Center for Physical and mental health, Mie University Graduate School of Medicine

# Equal contributed first author

Address for correspondence: Dr. Akiko Eguchi

Department of Gastroenterology and Hepatology, Mie University Graduate School of Medicine

2-174 Edobashi, Tsu, Mie, 514-8507, Japan

Tel: +81-59-231-9238

Email: akieguchi@med.mie-u.ac.jp

Running title: LCA effects on skeletal muscle hypertrophy

Funding: This research was supported by JSPS KAKENHI Grant Number 22K08011 and 21H02892, and AMED under Grant Number JP21fk0210090 and JP22fk0210115.

Conflict of Interest: The authors state no conflict of interest.

Key words: chronic liver diseases, low muscle mass, skeletal muscle, bile acids, lithocholic acid, liver-muscle axis.

Abbreviation: CLD; chronic liver disease, LCA; lithocholic acid, TGR5; G-protein-coupled receptor 5, BA; bile acid, BCAA; branched-amino acid, PMI; psoas muscle area index, IGF; insulin growth factor, mTOR; mammalian target of rapamycin; SMI, skeletal muscle index, CA; cholic acid, CDCA; chenodeoxycholic acid, DCA; deoxycholic acid, MHC; myosin heavy chain.

Abstract

[Background & aims] Hepatic sarcopenia is one of many complications associated with chronic liver disease (CLD) and has a high mortality rate, however, the liver-muscle axis is not fully understood. Therefore, few effective treatments exist for hepatic sarcopenia, the best of which being branched-amino acid (BCAA) supplementation to help increase muscle mass. Our aim was to investigate the molecular mechanism(s) of hepatic sarcopenia focused on bile acid (BA) composition. [Methods] Gastrocnemius muscle phenotype and serum BA levels were assessed in CLD rats treated with BCAA. Mouse skeletal muscle cells (C2C12) were incubated with lithocholic acid (LCA), G-protein-coupled receptor 5 (TGR5) agonist or TGR5 antagonist to assess skeletal muscle hypertrophy. The correlation between serum BA levels and psoas muscle area index (PMI) was examined in 73 CLD patients. [Results] Gastrocnemius muscle weight significantly increased in CLD rats treated with BCAA via suppression of protein degradation pathways, coupled with a significant increase in serum LCA levels. LCA treated C2C12 hypertrophy occurred in a concentration-dependent manner linked with TGR5-Akt pathways based upon inhibition results via a TGR5 antagonist. In human CLD, serum LCA levels were the sole factor positively correlated with PMI and were significantly decreased in both the low muscle mass group and the deceased group. Serum LCA levels were also shown to predict patient survival. [Conclusion] Our results indicate LCA-mediated skeletal muscle hypertrophy via activation of TGR5-IGF1-Akt signaling

pathways. In addition, serum LCA levels were associated with skeletal muscle mass in cirrhotic rats, as well as CLD patients, and predicted overall patient survival. [Funding] This research was supported by JSPS KAKENHI Grant Number 22K08011 and 21H02892, and AMED under Grant Number JP21fk0210090 and JP22fk0210115.

Introduction

Hepatic sarcopenia differs from aging sarcopenia insofar as it is defined by a rapid decrease in muscle mass and power. Hepatic sarcopenia is but one in the panoply of complications associated with chronic liver diseases (CLD), in particular liver cirrhosis with its high mortality (or low survival rate) and poor post-liver transplantation outcomes (Ebadi et al., 2019, Hara et al., 2016). A variety of factors are altered in hepatic sarcopenia, including decreased serum branched-chain amino acid (BCAA) levels (Tajiri and Shimizu, 2018), increased bile acids (BAs) (Kobayashi et al., 2017), abnormal insulin growth factor-1 (IGF-1) and mammalian target of rapamycin (mTOR) signaling pathways (Allen et al., 2021), increased reactive oxygen species and increased inflammatory cytokines and myostatin expression (Ebadi et al., 2019, Allen et al., 2021). BCAA supplementation has been shown to significantly improve skeletal muscle index measurements (Ismaiel et al., 2022). In contrast, anti-myostatin monoclonal neutralizing antibodies developed by several companies failed in clinical trials targeted to treat Duchenne muscular dystrophy (Wagner, 2020). The molecular mechanisms

75 underpinning the muscle-liver axis involved in hepatic sarcopenia are not fully understood.
76 Therefore, the elucidation of molecular mechanisms and effective treatment designs are
77 required to prevent the progression of hepatic sarcopenia and to improve overall patient
78 prognosis.
79 CLD has a major impact on BA composition (Sauerbruch et al., 2021). BAs are amphipathic
80 steroid molecules synthesized from cholesterol and are categorized as being primary or
81 secondary. Primary BAs are synthesized and conjugated in hepatocytes and secreted into
82 the intestine. Most conjugated BAs undergo deconjugation and dehydration by intestinal
83 bacteria, resulting in the production of secondary BAs. BA pools containing a mix of primary
84 and secondary BAs are essential for solubilizing lipids and fat-soluble vitamins thus
85 promoting their absorption into the small intestine. In addition to their canonical function in
86 digestion, BAs are known to act as signaling molecules that regulate metabolic pathways,
87 such as glucose, lipid and energy homeostasis, through various receptors including
88 G-protein-coupled receptor 5 (TGR5), farnesoid X receptor and vitamin D receptor (Arab et
89 al., 2017). TGR5 activation induced by cholic acid (CA), chenodeoxycholic acid (CDCA),
90 deoxycholic acid (DCA) and lithocholic acid (LCA) as part of the overall BA composition is a
91 key event regulating skeletal muscle cells with the most potent endogenous ligand for TGR5
92 being LCA (Pols et al., 2011). Indeed, LCA, a secondary BA, induced TGR5 activation in
93 skeletal muscle and enhanced muscle mass hypertrophy in mice through an increase in

IGF-1, a known muscle hypertrophy-related gene (Sasaki et al., 2018). However, the role of LCA in cirrhotic liver disease-related sarcopenia has not been fully clarified.

In this study, we investigate the interaction between BAs, including LCA, and skeletal muscle mass, in CLD rats, as well as CLD patients, and explore the beneficial effect of LCA on skeletal muscle hypertrophy.

Results

Increased gastrocnemius muscle weight is associated with suppression of protein degradation pathways and elevation of serum LCA levels in CLD rats treated with BCAA.

To investigate whether increased gastrocnemius muscle weight is associated with changes in BA composition, we used a CLD rat model administered with carbontetrachloride (CCl_4) for 10 weeks (4 weeks to establish advanced fibrosis, or cirrhosis, and an additional 6 weeks to treat with BCAA for attenuation of liver injury), which we have previously reported (Tamai et al., 2021). The ratio of gastrocnemius muscle weight to total body weight was significantly increased in CLD rats treated with BCAA (CLD+BCAA) compared to untreated CLD rats ($p < 0.05$) (Figure. 1A). The overall pathological condition of gastrocnemius muscle was similar between CLD and CLD+BCAA rats (Figure. 1B). Moreover, in concordance with the aforementioned gastrocnemius muscle mass results, gastrocnemius muscle gene expression

levels of protein degradation pathways including muscle RING finger 1 (MuRF1), muscle atrophy F-box protein (MafBx), ubiquitin and E214KDa were notably increased in CLD rats compared with normal rats (indicated as a broken line in the graphs) and MafBx mRNA levels were significantly decreased in gastrocnemius muscle from CLD+BCAA rats ($p < 0.05$) (Figure. 1C). The mRNA levels of the repair gene, transcription factor forkhead box O1 (FOXO1), were notably decreased in CLD rat gastrocnemius muscle samples, but expression recovered in gastrocnemius muscle samples from CLD+BCAA rats (Figure. 1C). To explore whether increased gastrocnemius muscle mass was associated with BA composition, we measured serum BA levels in CLD and CLD+BCAA rats. Total BAs were dramatically increased in CLD rats when compared to normal rats (indicated as a broken line in a graph) and decreased in CLD+BCAA rats (Figure. 1D). In line with the total BA data, the ratio of CA, CDCA and DCA increased in CLD rats and showed a decreasing trend in CLD+BCAA rats (Figure. 1E). Notably, the ratio of LCA to total BAs was dramatically decreased in CLD rats and was significantly increased in the CLD+BCAA rat group ($p < 0.05$) (Figure. 1E). These results suggest that an increase in gastrocnemius muscle mass may be associated with serum LCA levels.

LCA enhances muscle cell hypertrophy through TGR5-IGF-1 pathway.

We next examined the effect of LCA on hypertrophy of skeletal muscle cells using C2C12 myoblasts that differentiate rapidly forming myotubes. C2C12 myoblasts were culture for 3 days and approached confluence, then differentiated to myotubes using varying concentrations of LCA (Figure. 2A). The hypertrophy of C2C12 myotubes was overtly altered in a concentration-dependent manner based on assessment using myosin heavy chain (MHC) staining (Figure. 2B). Corresponding to cell morphological changes, the length and width of the cells were significantly increased in a concentration-dependent manner under quantitative analyses (length, $p < 0.001$: 0 vs. 700 nM and 70 vs. 700 nM, $p < 0.01$: 0 and 70 nM) (width, $p < 0.001$: 0 vs. 70 or 700 nM and 70 vs. 700 nM) (Figure. 2C). Previous reports have shown LCA to be one of the most potent endogenous ligands for TGR5 (Pols et al., 2011) capable of inducing IGF-1, which is a known muscle hypertrophy gene (Sasaki et al., 2018). In the present study, we found the levels of *Tgr5* mRNA to be significantly increased in C2C12 myotubes treated with LCA ($p < 0.05$: 70 and 700 nM) (Figure. 2D). Moreover, C2C12 myotubes undergoing LCA-induced hypertrophy showed significantly elevated levels of *Igf-1* mRNA (Figure. 2D).

TGR5 agonist accelerates muscle cell hypertrophy through IGF-1 and Akt activation.

To investigate whether LCA-induced TGR5-IGF-1 activation is attenuated by blocking the TGR5 pathway, C2C12 myotubes were coincubated with LCA and TGR5 antagonist

(SBI-115). The mRNA levels of *Tgr5* and *Igf-1* were significantly decreased in C2C12 myotubes treated with LCA+SBI-115 compared to LCA alone ($p < 0.01$ and $p < 0.05$, respectively) (Figure. 3A). LCA is the most potent endogenous ligand for TGR5, but also cytotoxic (Pols et al., 2011), therefore, LCA alone may not be an appropriate therapeutic target molecule. A TGR5 agonist (INT-777) has been generated and shown to be a useful molecule for TGR5 activation (Pellicciari et al., 2009). To explore whether this TGR5 agonist induces muscle cell hypertrophy, differentiated C2C12 myoblasts (myotubes) were incubated with INT-777. INT-777 induced obvious muscle cell hypertrophy when assessed using MHC staining (Figure. 3B). INT-777 also elevated the mRNA levels of *Tgr5* and *Igf1* ($p < 0.01$ an $p < 0.001$, respectively) (Figure. 3C). IGF-1 is known to activate the PI3K-Akt pathway, thus leading to stimulation of protein synthesis, resulting in accelerated muscle hypertrophy (Sartori et al., 2021). Indeed, the ratio of Akt phosphorylation against to total Akt was significantly increased in C2C12 myotubes treated with INT-777 (Figure. 3D). These results suggest that the TGR5-IGF-1-Akt3 pathway contributes to muscle hypertrophy.

Serum LCA levels are positively and significantly correlated with PMI in CLD patients.

The clinical features of the 73 (58 men and 15 women) enrolled CLD patients are shown in Table 1. The cohort of patients admitted to our study was based on a variety of causative agents: 13 hepatitis B virus (HBV), 21 hepatitis C virus (HCV), 21 nonalcoholic steatohepatitis

169 (NASH), 16 alcoholism and 2 other factors. Patients infected with HBV or HCV were under
170 infection control, with sustained virological response monitoring, by direct-acting antiviral
171 treatment against HCV, or treatment with nucleos(t)ide analogs against HBV in the clinical
172 course of each patient. The Barcelona Clinic Liver Cancer (BCLC) staging showed 11, 29, 13,
173 19 and 1 patients in Stage 0, A, B, C, and D, respectively.
174 The patient mean of total serum BAs was 18.3 ± 17.0 μmol/L, composed of primary BAs (12.7
175 ± 14.0 μmol/L) and secondary BAs (5.58 ± 7.91 μmol/L). The serum level of 15 individual BA
176 compositions are shown in Table 2. Total serum primary BA level was negatively correlated
177 with albumin ($r = -0.456$, $p < 0.0001$) and prothrombin time (PT, %) ($r = -0.410$, $p < 0.001$) and
178 was positively correlated with alkaline phosphatase (ALP) ($r = 0.240$, $p < 0.05$) (Figure. 4A).
179 Furthermore, the total primary BA level was significantly higher in albumin-bilirubin (ALBI)
180 grade 2 and 3 than in ALBI grade 1 ($p < 0.001$) (Figure. 4B). Notably, psoas muscle area
181 index (PMI) values were positively and significantly correlated with serum LCA levels (r
182 $= 0.304$, $p < 0.01$) and serum LCA ratio, which was LCA/total BAs ($r = 0.230$, $p < 0.05$), and the
183 only BA composition correlated with PMI (Figure. 4C). Next, we set out to assess the
184 changes in serum BA composition associated with muscle mass. To do this the cohort was
185 divided into two groups: low muscle mass, defined by PMI below 6.36 cm^2/m^2 for men and
186 3.92 cm^2/m^2 for women (Hamaguchi et al., 2016), and normal muscle mass. The level of total
187 primary BAs was decreased and total secondary BAs was increased in the low muscle mass

group compared with the normal muscle mass group (Figure. 4D). The level of serum TGR5 ligands, CA, CDCA, DCA and LCA were also decreased in the low muscle mass group (Figure. 4D). In particular, the level of serum LCA was significantly decreased in the low muscle mass group (Figure. 4D). These results show that serum LCA levels are indicative of overall muscle mass in CLD patients.

Serum LCA levels may be a prognostic factor for survival.

Finally, we investigated the association between serum BA composition levels and survival. 23 out of 73 patients (31.5 %) died in the average follow-up period of 1005 ± 471 days following our study period. Serum total primary BA levels were significantly elevated in the deceased group ($p < 0.05$), while serum LCA levels were significantly decreased in the deceased group compared to the survival group ($p < 0.05$) (Figure. 5A). ROC analyses concerning predictors of survival yielded AUC values of 0.670 (95% confidence interval: 0.542-0.797) ($p < 0.05$) for total primary BAs and 0.649 (95% confidence interval: 0.519-0.779) ($p < 0.05$) for LCA (Figure. 5B). In the present study, we calculated the ROC analysis survival curve cut-off values for total primary BAs at 10.5 μmol/L (sensitivity 69.6% and specificity 68.0%) and LCA at 0.32 μmol/L (sensitivity 73.9% and specificity 60%). Patients with low total primary BAs (<10.5) showed significantly better OS than patients with high total primary BAs ($p < 0.01$) (Figure. 5C). Furthermore, patients with high LCA (≥0.32)

showed significantly improved OS than patients with low LCA ($p < 0.01$) (Figure. 5C). These results suggest that serum LCA levels can be useful in predicting patient survival.

Discussion

In the present study, we demonstrated that serum LCA levels and LCA ratio were positively associated with skeletal muscle mass in CLD rats treated with BCAA, as well as human subjects, and that LCA-induced skeletal muscle cell hypertrophy occurs through TGR5-IGF-1-Akt3 activation. BCAA supplementation is approved for use in CLD patients within the clinical setting as a means to provide compensatory albumin thus maintaining liver function (European Association for the Study of the Liver. Electronic address and European Association for the Study of the, 2019), as well as increased muscle mass associated with an acceleration of the TCA cycle (Ismaiel et al., 2022). In our previous study, we reported that hepatocellular damage was attenuated using BCAA supplementation as a result of improved lipid metabolism and mitochondrial damage repair in CLD rats (Tamai et al., 2021). Using the same CLD rat model in the current study, we revealed that gastrocnemius muscle mass was significantly increased using BCAA treatment. BCAA treatment has direct effects on liver and skeletal muscle, however we hypothesized that one or more CLD-related molecules/factors might regulate skeletal muscle mass via a liver-muscle axis. Indeed, we found that the serum LCA ratio (LCA/total BAs) was significantly increased in CLD rats, which also showed an

226 increase in gastrocnemius muscle mass. Furthermore, we showed that serum LCA and LCA
227 ratio were significantly and positively associated with PMI in CLD patients. These results from
228 CLD rats and human subjects suggest that LCA can regulate muscle mass via a liver-muscle
229 axis, although further studies are warranted in the future using a greater number of patients
230 as part of a multicenter study.

231 The role of LCA in the progression of CLD has not been fully developed due to the lack of
232 general sensitivity in the system used to measure BA composition and is therefore not
233 sufficient to detect low levels of LCA in the blood. Our established highly-sensitive system for
234 BA composition (Murakami et al., 2018) allows us to detect all aspects of BA composition
235 resulting in the discovery of a new role for LCA, which is a positive correlation of serum BA
236 composition with skeletal muscle mass in CLD patients. Furthermore, we revealed that a
237 decrease in serum LCA level portends a worse survival outcome in CLD patients with
238 associated low muscle mass. CLD patients with sarcopenia, defined by low muscle mass and
239 power, also display decreased survival when compared to CLD patients without sarcopenia
240 (Hara et al., 2016), thus serum LCA may be a useful measure to monitor sarcopenia in CLD
241 patients. Current reports have also demonstrated that LCA is one of the most potent
242 anti-bacterial agents, selective against gram-positive bacteria, resulting in a longer lifespan of
243 centenarians (Sato et al., 2021) and is one of the most potent endogenous ligands for TGR5,
244 which protects against alcohol-induced liver steatosis and inflammation in mice

(Iracheta-Vellve et al., 2018). This evidence clearly shows that LCA plays a critical role in the progression of CLD, and intestinal microbiota, as a function of the liver-gut axis. Our latest results presented here, associating LCA with skeletal muscle mass, will lead to new insights into the role of LCA as a component of the liver-muscle-gut axis.

In CLD rats and human subjects, we observed an association between gastrocnemius muscle mass and LCA only, although serum CA, CDCA and DCA levels also showed a decreasing trend in CLD patients with low muscle mass. This result is reasonable since the hierarchy of BA affinity for TGR5 is as follows: LCA > DCA > CDCA > CA (Sato et al., 2007). We also demonstrated that a TGR5 antagonist induced skeletal muscle cell hypertrophy through IGF-1 activation, but we need further studies to develop a new antagonist with similar affinity of LCA to the TGR5 binding pocket minus the cytotoxicity aspect.

In conclusion, we revealed new roles for LCA as a positive regulator of skeletal muscle mass in both CLD rats and human patients, and as a mediator of skeletal muscle cell hypertrophy in differentiated C2C12 myoblasts (myotubes). The serum LCA ratio measurement was significantly decreased in CLD patients with low muscle mass. Current results suggest that serum LCA levels may be used as a prognostic factor of survival in CLD patients with sarcopenia, and a TGR5 agonist holds the potential to be a candidate as a therapeutic target in the prevention of sarcopenia in CLD patients.

Methods

Animal samples

Our animal protocol (HKD43046) was reviewed and approved by the Institutional Animal Care and Use Committee at Hokudo Co., Ltd (Sapporo, Japan). The rat model of CLD has been previously described in detail (Tamai et al., 2021). Briefly, Wister male rats (SPF, CLEA Japan: Tokyo, Japan) aged 7 weeks were fed solid normal diet, CE-2 (CLEA Japan), under conventional conditions and were orally administered CCl_4 at 1.0 mL/kg twice a week for 4 weeks to induce advanced fibrosis, or cirrhosis, at which point the animals were divided into 2 groups by weight stratified random sampling. The CLD rats then received daily oral administration of BCAA (10 g/kg/day) (n =10), or 0.9% saline solution (control) (n =10) for 6 weeks. The CLD state was maintained with twice weekly administration of CCl_4 at 0.5 mL/kg for 6 weeks (10 weeks total). The rats were individually maintained at a constant temperature (23 ± 3 °C), 50 ± 20% relative humidity and 12 h light–dark cycles (lights on at 7 am), and had free access to food and water. Analysis of rat number was 9/10 in BCAA group and 8/10 in control group due to death by CCl_4 in the experimental term. Wister male rats aged 10 weeks were used as a control, wild-type rats (n=3).

Gastrocnemius muscle histological analysis and serum BA measurement in rats

All rats were sacrificed at the conclusion of our treatment protocol under anesthesia (isoflurane, DS-pharma, Osaka, Japan). Whole rat blood was collected and allocated into tubes with anticoagulant (EDTA). A portion of gastrocnemius muscle was fixed in 10% formalin for 24 h and embedded in paraffin and the remaining gastrocnemius muscle was flash frozen in liquid nitrogen and stored at -80˚C. The gastrocnemius muscle sections were prepared and stained for H&E (hematoxylin and eosin). All images were taken by Olympus CKX53 (Olympus, Tokyo, Japan) and quantitated using Image J software (NIH Image). Serum BA levels were quantified by LC-MS/MS at CMIC Pharma Science Co., Ltd. (Kobe, Japan).

Patients and serum BA measurements in human

The study protocol (H2019-063) was approved by the Clinical Research Ethics Review Committee of Mie University Hospital. This study was performed retrospectively on stored samples, and subjects were allowed to opt out of their data being used. Written informed consent was obtained from all subjects at the time of blood sampling. A total of 113 treatment-naïve patients with hepatocellular carcinoma (HCC) hospitalized in the Department of Gastroenterology and Hepatology, Mie University Hospital for treatment of HCC between January 2015 and January 2017 were included as a retrospective study. HCC diagnosis was based on clinical history, serologic testing and radiologic imaging. 36 patients were excluded

301 due to oral administration of ursodeoxycholic acid. Three patients who had other
302 malignancies within the past 3 years were excluded. One patient was excluded due to kidney
303 transplant. As a result, a total of 73 patients with CLD were analyzed for the current study.
304 Patients positive for hepatitis B surface antigen were diagnosed with HBV infection, whereas
305 those positive for anti-HCV were diagnosed with HCV infection. Alcohol associated liver
306 disease was defined as alcohol consumption >60g/day. NASH was diagnosed based on
307 pathological findings and/or fatty liver without any other evident causes of chronic liver
308 diseases (viral, autoimmune, genetic, etc.). Hepatic functional reserve was categorized by
309 ALBI score (Johnson et al., 2015). The PMI [psoas muscle area at the middle of the third
310 lumbar vertebra (L3) (cm^2)/height $(m)^2$] was manually calculated from CT images. All
311 treatments were performed following the Japanese practical guidelines for HCC as possible
312 (Kokudo et al., 2019). Post-HCC treatment follow-up consisted of laboratory tests, including
313 tumor markers, every 3 months and dynamic CT or magnetic resonance imaging every 6
314 months.
315 BA concentrations were determined in a blind as described by Ando et al. with minor
316 modifications (Murakami et al., 2018, Ando et al., 2006). After the addition of internal
317 standards and 0.5 M potassium phosphate buffer (pH 7.4), BAs were extracted with Bond
318 Elut C18 cartridges and quantified by LC-MS/MS. Chromatographic separation was
319 performed using a Hypersil GOLD column (150 × 2.1 mm, 3.0 μm; Thermo Fisher Scientific)

320 at 40°C. The mobile phase consisted of (A) 20 mM ammonium acetate buffer (pH
321 7.5)-acetonitrile-methanol (70:15:15, v/v/v) and (B) 20 mM ammonium acetate buffer (pH
322 7.5)-acetonitrile-methanol (30:35:35, v/v/v). The following gradient program was used at a
323 flow rate of 200 µl/min: 0–100% B for 20 min, hold 100% B for 10 min, and re-equilibrate to
324 100% A for 8 min.
325
326 **Cell culture, treatment and immunofluorescence**
327 C2C12 myoblasts (kindly gift from Dr. Fujita at Tokyo institute of Technology) were
328 maintained in DMEM containing 20% FBS at 37 ˚C and 5% CO_2. The confluent cells were
329 differentiated into myotubes by culturing with DMEM containing 2% horse serum for 5 days
330 with LCA (Millipore-Sigma, Japan), TGR5 agonist (1 µM INT-777, Millipore-Sigma) or TGR5
331 agonist plus TGR5 antagonist (100 µM SBI-115, Millipore-Sigma). All experiments were
332 repeated twice with three biological replicates in each experiment. For immunofluorescence,
333 cells were fixed with 4% paraformaldehyde for 10 min, permeabilized with 0.5% Triton X-100
334 for 5min and then incubated with anti-MHC antibody (#376157, Santa Cruz, Dallas, TX) at 4
335 ˚C overnight. MHC and nucleus were visualized with Alexa 488-conjugated anti-mouse
336 antibody and DAPI, respectively. All pictures were taken by KEENC BZ-X710 (KEYENCE,
337 Japan). Changes in cell strength and width were quantified using NIH ImageJ software.
338

Gene expression

Total RNA was isolated from gastrocnemius muscle or C2C12 cells using TRI Reagent (Molecular Research Center, Cincinnati, OH) according to the manufacturer's instructions. The cDNA was synthesized from total RNA using a cDNA Synthesis kit (Takara, Shiga, Japan). Real-time PCR quantification was performed using the KAPA SYBR FAST qPCR master mix (KAPA Biosystems, Wilmington, MA) or a TaqMan gene expression assay (Thermo Fisher Scientific Inc.) for *Sod1*, and the 7300 Real-Time PCR Detection System (Thermo Fisher Scientific Inc.). The PCR primers were used to amplify each gene as listed in Supplemental Table 1. Mean values of mRNA were normalized to *beta 2 microglobulin (B2m)*.

Western Blotting Analysis

C2C12 cells were homogenized in RIPA buffer (150 mM NaCl, 1.0% NP-40, 1% sodium deoxycholate, 0.1% sodium dodecyl sulphate, 50 mM Tris-HCl pH8.0) containing a protease inhibitor cocktail (Millipore-Sigma) and phosphatase inhibitors (Millipore-Sigma). 20 μg of cell lysate was resolved using a TGX gel (Bio-Rad, Hercules, CA), transferred to a polyvinylidenedifluoride membrane, and blotted with the appropriate primary antibody. Membranes were incubated with peroxidase-conjugated secondary antibody (GE Healthcare Bioscience, Marlborough, MA). Protein bands were visualized using an

enhanced chemiluminescence reagent (Bio-Rad), digitized using a Lumino-image analyzer (LAS-4000 iniEPUV, Fuji Film, Tokyo, Japan), and quantitated using the program Multi Gauge (Fuji Film). Anti-GAPDH (#60004, Proteintech, Rosemont, IL), anti-phospho-Akt (Ser 473) (#4060, Cell Signaling Technology, Danvers, MA) and anti-pan-Akt (#4691, Cell Signaling Technology) were used as primary antibodies.

Statistical analyses

Continuous variables are presented as mean ± standard deviation or median (minimum-maximum), and categorical variables are shown as numbers of patients. The continuous data were compared using the Mann-Whitney U or unpaired t test in two groups or Kruskal-Wallis in multiple groups. The relationship between the serum BA levels and clinical data were examined using Spearman's rank correlation coefficient. The categorical data were compared using the Chi-squared test. Receiver operator characteristic (ROC) curves and the corresponding area under the curve (AUC) were used to obtain cut-offs for the outcomes. The Youden index was applied to calculate the optimal cut-off point. Overall survival (OS) was measured using the Kaplan-Meier method and compared using the log-rank test. All statistical analyses were performed using SPSS23.0 software (IBM, Armonk, NY) or Prism 9 (GraphPad Software, Inc., CA, USA). Differences were considered to be significant at $p < 0.05$.

Acknowledgement

We would like to thank Dr. Teruo Miyazaki, Dr. Akira Honda and Dr. Tadashi Ikegami in Department of Gastroenterology, Tokyo Medical University Ibaraki medical center for measurement of human BAs.

References

ALLEN, S. L., QUINLAN, J. I., DHALIWAL, A., ARMSTRONG, M. J., ELSHARKAWY, A. M., GREIG, C. A., LORD, J. M., LAVERY, G. G. & BREEN, L. 2021. Sarcopenia in chronic liver disease: mechanisms and countermeasures. *Am J Physiol Gastrointest Liver Physiol,* 320**,** G241-G257.

ANDO, M., KANEKO, T., WATANABE, R., KIKUCHI, S., GOTO, T., IIDA, T., HISHINUMA, T., MANO, N. & GOTO, J. 2006. High sensitive analysis of rat serum bile acids by liquid chromatography/electrospray ionization tandem mass spectrometry. *J Pharm Biomed Anal,* 40**,** 1179-86.

ARAB, J. P., KARPEN, S. J., DAWSON, P. A., ARRESE, M. & TRAUNER, M. 2017. Bile acids and nonalcoholic fatty liver disease: Molecular insights and therapeutic perspectives. *Hepatology,* 65**,** 350-362.

EBADI, M., BHANJI, R. A., MAZURAK, V. C. & MONTANO-LOZA, A. J. 2019. Sarcopenia in cirrhosis: from pathogenesis to interventions. *J Gastroenterol,* 54**,** 845-859.

EUROPEAN ASSOCIATION FOR THE STUDY OF THE LIVER. ELECTRONIC ADDRESS, E. E. E. & EUROPEAN ASSOCIATION FOR THE STUDY OF THE, L. 2019. EASL Clinical Practice Guidelines on nutrition in chronic liver disease. *J Hepatol,* 70**,** 172-193.

HAMAGUCHI, Y., KAIDO, T., OKUMURA, S., KOBAYASHI, A., HAMMAD, A., TAMAI, Y., INAGAKI, N. & UEMOTO, S. 2016. Proposal for new diagnostic criteria for low skeletal muscle mass based on computed tomography imaging in Asian adults. *Nutrition,* 32**,** 1200-5.

HARA, N., IWASA, M., SUGIMOTO, R., MIFUJI-MOROKA, R., YOSHIKAWA, K., TERASAKA, E., HATTORI, A., ISHIDOME, M., KOBAYASHI, Y., HASEGAWA, H., IWATA, K. & TAKEI, Y. 2016. Sarcopenia and Sarcopenic Obesity Are Prognostic Factors for Overall Survival in Patients with Cirrhosis. *Intern Med,* 55**,** 863-70.

IRACHETA-VELLVE, A., CALENDA, C. D., PETRASEK, J., AMBADE, A., KODYS, K., ADORINI, L. & SZABO, G. 2018. FXR and TGR5 Agonists Ameliorate Liver Injury, Steatosis, and Inflammation After Binge or Prolonged Alcohol Feeding in Mice.

Hepatol Commun, 2**,** 1379-1391.
ISMAIEL, A., BUCSA, C., FARCAS, A., LEUCUTA, D. C., POPA, S. L. & DUMITRASCU, D. L. 2022. Effects of Branched-Chain Amino Acids on Parameters Evaluating Sarcopenia in Liver Cirrhosis: Systematic Review and Meta-Analysis. *Front Nutr,* 9**,** 749969.
JOHNSON, P. J., BERHANE, S., KAGEBAYASHI, C., SATOMURA, S., TENG, M., REEVES, H. L., O'BEIRNE, J., FOX, R., SKOWRONSKA, A., PALMER, D., YEO, W., MO, F., LAI, P., INARRAIRAEGUI, M., CHAN, S. L., SANGRO, B., MIKSAD, R., TADA, T., KUMADA, T. & TOYODA, H. 2015. Assessment of liver function in patients with hepatocellular carcinoma: a new evidence-based approach-the ALBI grade. *J Clin Oncol,* 33**,** 550-8.
KOBAYASHI, Y., HARA, N., SUGIMOTO, R., MIFUJI-MOROKA, R., TANAKA, H., EGUCHI, A., IWASA, M., HASEGAWA, H., IWATA, K., TAKEI, Y. & TAGUCHI, O. 2017. The Associations between Circulating Bile Acids and the Muscle Volume in Patients with Non-alcoholic Fatty Liver Disease (NAFLD). *Intern Med,* 56**,** 755-762.
KOKUDO, N., TAKEMURA, N., HASEGAWA, K., TAKAYAMA, T., KUBO, S., SHIMADA, M., NAGANO, H., HATANO, E., IZUMI, N., KANEKO, S., KUDO, M., IIJIMA, H., GENDA, T., TATEISHI, R., TORIMURA, T., IGAKI, H., KOBAYASHI, S., SAKURAI, H., MURAKAMI, T., WATADANI, T. & MATSUYAMA, Y. 2019. Clinical practice guidelines for hepatocellular carcinoma: The Japan Society of Hepatology 2017 (4th JSH-HCC guidelines) 2019 update. *Hepatol Res,* 49**,** 1109-1113.
MURAKAMI, M., IWAMOTO, J., HONDA, A., TSUJI, T., TAMAMUSHI, M., UEDA, H., MONMA, T., KONISHI, N., YARA, S., HIRAYAMA, T., MIYAZAKI, T., SAITO, Y., IKEGAMI, T. & MATSUZAKI, Y. 2018. Detection of Gut Dysbiosis due to Reduced Clostridium Subcluster XIVa Using the Fecal or Serum Bile Acid Profile. *Inflamm Bowel Dis,* 24**,** 1035-1044.
PELLICCIARI, R., GIOIELLO, A., MACCHIARULO, A., THOMAS, C., ROSATELLI, E., NATALINI, B., SARDELLA, R., PRUZANSKI, M., RODA, A., PASTORINI, E., SCHOONJANS, K. & AUWERX, J. 2009. Discovery of 6alpha-ethyl-23(S)-methylcholic acid (S-EMCA, INT-777) as a potent and selective agonist for the TGR5 receptor, a novel target for diabesity. *J Med Chem,* 52**,** 7958-61.
POLS, T. W., NORIEGA, L. G., NOMURA, M., AUWERX, J. & SCHOONJANS, K. 2011. The bile acid membrane receptor TGR5: a valuable metabolic target. *Dig Dis,* 29**,** 37-44.
SARTORI, R., ROMANELLO, V. & SANDRI, M. 2021. Mechanisms of muscle atrophy and hypertrophy: implications in health and disease. *Nat Commun,* 12**,** 330.
SASAKI, T., KUBOYAMA, A., MITA, M., MURATA, S., SHIMIZU, M., INOUE, J., MORI, K. & SATO, R. 2018. The exercise-inducible bile acid receptor Tgr5 improves skeletal muscle function in mice. *J Biol Chem,* 293**,** 10322-10332.
SATO, H., GENET, C., STREHLE, A., THOMAS, C., LOBSTEIN, A., WAGNER, A.,

MIOSKOWSKI, C., AUWERX, J. & SALADIN, R. 2007. Anti-hyperglycemic activity of a TGR5 agonist isolated from Olea europaea. *Biochem Biophys Res Commun,* 362**,** 793-8.

SATO, Y., ATARASHI, K., PLICHTA, D. R., ARAI, Y., SASAJIMA, S., KEARNEY, S. M., SUDA, W., TAKESHITA, K., SASAKI, T., OKAMOTO, S., SKELLY, A. N., OKAMURA, Y., VLAMAKIS, H., LI, Y., TANOUE, T., TAKEI, H., NITTONO, H., NARUSHIMA, S., IRIE, J., ITOH, H., MORIYA, K., SUGIURA, Y., SUEMATSU, M., MORITOKI, N., SHIBATA, S., LITTMAN, D. R., FISCHBACH, M. A., UWAMINO, Y., INOUE, T., HONDA, A., HATTORI, M., MURAI, T., XAVIER, R. J., HIROSE, N. & HONDA, K. 2021. Novel bile acid biosynthetic pathways are enriched in the microbiome of centenarians. *Nature,* 599**,** 458-464.

SAUERBRUCH, T., HENNENBERG, M., TREBICKA, J. & BEUERS, U. 2021. Bile Acids, Liver Cirrhosis, and Extrahepatic Vascular Dysfunction. *Front Physiol,* 12**,** 718783.

TAJIRI, K. & SHIMIZU, Y. 2018. Branched-chain amino acids in liver diseases. *Transl Gastroenterol Hepatol,* 3**,** 47.

TAMAI, Y., CHEN, Z., WU, Y., OKABE, J., KOBAYASHI, Y., CHIBA, H., HUI, S. P., EGUCHI, A., IWASA, M., ITO, M. & TAKEI, Y. 2021. Branched-chain amino acids and l-carnitine attenuate lipotoxic hepatocellular damage in rat cirrhotic liver. *Biomed Pharmacother,* 135**,** 111181.

WAGNER, K. R. 2020. The elusive promise of myostatin inhibition for muscular dystrophy. *Curr Opin Neurol,* 33**,** 621-628.

Figure legends

Figure 1. Gastrocnemius muscle mass and serum LCA ratio are significantly increased in CLD rats treated with BCAA. (A) Changes in gastrocnemius muscle/body weight in CLD rats (n=9) and CLD rats treated with BCAA (CLD+BCAA)(n=8). (B) Hematoxylin & Eosin (H&E) staining in gastrocnemius muscle sections from CLD and CLD+BCAA rats. Scale bar, 50 μm. (C) Gene expression of *MuRF1*, *MafBx*, *ubiquitin*, *E214KDa* and *FOXO1* in gastrocnemius muscle from CLD and CLD+BCAA rats as measured by qPCR. All gene expression levels were normalized to housekeeping control, *β2 microglobulin*, and shown

480 relative to the expression levels of control (normal rats). Broken line indicates the expression
481 levels of gastrocnemius muscle from normal rats. (D, E) Changes in (C) serum total BAs, (D)
482 CA/total BAs, CDCA/total BAs, DCA/total BAs and LCA/total BAs in CLD and CLD+BCAA
483 rats. Broken line indicates the serum BA levels from normal rats.*p<0.05. Values are mean ±
484 SEM. CLD; chronic liver disease, MuRF1; muscle RING finger 1, MafBx; muscle atrophy
485 F-box protein, FOXO1; forkhead box O1, BAs; bile acids, CA; cholic acid, CDCA;
486 chenodeoxycholic acid, DCA; deoxycholic acid, LCA; lithocholic acid.
487
488 **Figure 2. LCA induces hypertrophy of skeletal muscle cells.** (A) Scheme of experimental
489 design in C2C12 myoblast to myotubes treated with LCA. (B) Myosin heavy chain (MHC)
490 staining in C2C12 myotubes treated with 0, 70 and 700 nM of LCA. Scale bar, 50 μm. (C)
491 Changes in length and width of MHC positive cells quantified from Figure 2B. (D) Gene
492 expression of *Tgr5* and *Igf-1* in C2C12 myotubes treated with 0, 70 and 700 nM of LCA.
493 ****p<0.0001, **p<0.01, *p<0.05. Values are mean ± SEM from three biological replicates.
494 LCA; lithocholic acid, TGR5; G-protein-coupled receptor 5, IGF; insulin growth factor.
495
496 **Figure 3. Hypertrophy of skeletal muscle cells is induced by TGR5-IGF-1-Akt3**
497 **activation.** (A) Gene expression of *Tgr5* and *Igf-1* in C2C12 myotubes treated with 70 nM
498 LCA and 70 nM LCA plus 100 μM of TGR5 antagonist, SBI-115. (B) Myosin heavy chain

(MHC) staining in C2C12 myotubes treated with 1 μM of TGR5 agonist, INT-777. Scale bar, 50 μm. (C) Gene expression of *Tgr5* and *Igf-1* in C2C12 myotubes treated with 1 μM of INT-777. (D) Protein expression of phosphorylated Akt3 (p-Akt3), Akt3 and GAPDH measured by western blotting in C2C12 myotubes treated with 1 μM of INT-777. Quantification of pAkt3/Akt3 from western blotting membrane. ***p<0.001, **p<0.01, *p<0.05. Values are mean ± SEM from three biological replicates. LCA; lithocholic acid, TGR5; G-protein-coupled receptor 5, IGF; insulin growth factor; Akt3; AKT serine/threonine kinase 3, GAPDH; glyceraldehyde-3-phosphate dehydrogenase.

Figure 4. Serum LCA level is significantly and positively correlated with PMI in CLD patients and is significantly decreased in CLD patients with low muscle mass. (A) Correlation between total primary BAs and Albumin (ALB), alkaline phosphatase (ALP) or prothrombin time (PT) (%) in CLD patients. (B) Changes in total primary BAs in CLD patients with ALBI grade 1 or grade 2-3. (C) Correlation of Psoas muscle mass index (PMI) with serum LCA and LCA ratio in CLD patients. (D) Changes in total serum primary BAs, total secondary BAs, CA, CDCA, DCA and LCA in CLD patients with normal muscle mass and low muscle mass. ***p<0.001, *p<0.05. Values are mean ± SEM. CLD; chronic liver disease, BAs; bile acids, ALBI; albumin-bilirubin, CA; cholic acid, CDCA; chenodeoxycholic acid, DCA; deoxycholic acid, LCA; lithocholic acid.

Figure 5. Improved survival in CLD patients with high levels of serum LCA. (A) Serum total of primary BAs and LCA ratio in survival and deceased CLD patients. (B) ROC curve of serum total or primary BAs and LCA. (C) CLD patient survival curve with total primary BAs and LCA. Correlation of Psoas muscle mass index (PMI) with serum LCA and LCA ratio in CLD patients. *p<0.05. Values are mean ± SEM. BAs; bile acids, LCA; lithocholic acid, AUC; area under the curve.

Figure 1-source data. Ratio of gastrocnemius weight/body weight in CLD rats and CLD rats treated with BCAA (CLD+BCAA). Serum total BAs, CA/total BAs, CDCA/total BAs, DCA/total BAs and LCA/total BAs in CLD and CLD+BCAA rats.

Figure 2-source data. Ratio of length and width of MHC positive cells quantified from myosin heavy chain (MHC) staining in C2C12 myotubes treated with 0, 70 and 700 nM of LCA.

Figure 3-source data. Original membrane of immunoblotting.

Figure 4-source data. Serum total primary BAs, albumin (ALB), alkaline phosphatase (ALP), prothrombin time (PT) (%), psoas muscle mass index (PMI), LCA and LCA ratio in CLD patients. Serum total serum primary BAs, total secondary BAs, CA, CDCA, DCA and LCA in CLD patients with normal muscle mass and low muscle mass.

Figure 5-source data. Serum total of primary BAs and LCA ratio in survival and deceased CLD patients. CLD patient survival curve with total primary BAs and LCA.

Table 1-source data. Serum albumin, total bilirubin, ALBI, prothrombin time and PMI in CLD patients.

Table 2-source data. Serum total BAs, total primary BAs, total secondary BAs and bile acids composition in CLD patients.

Table 1. CLD patient baseline clinical and biochemical profiles of CLD patients.

	n=73
Age, years	71.0±11.0
Gender, male/female	58/15
Etiology, HBV/HCV/NASH/alcohol/others	13/21/21/16/2
BCLC (0/A/B/C/D)	11/29/13/19/1
Albumin, g/dl	4.04±0.49
Total bilirubin, mg/dl	1.00±0.53
ALBI	-2.65±0.48
Prothrombin time, %	87.6±18.7
PMI, cm^2/m^2	5.13±1.99

Data are presented as number of patients, mean ± standard deviation.
CLD; chronic liver disease, HBV; hepatitis B virus, HCV; hepatitis C virus, NASH; nonalcoholic steato hepatitis, ALBI: The albumin-bilirubin, PMI: psoas mass index.

Table 2. Baseline bile acids composition.

	n=73 (mmol/L)
Total bile acids	18.3±17.0
Total of primary bile acids	12.7±14.0
CA	1.30±3.28
GCA	1.71±2.86
TCA	0.35±0.78
CDCA	2.68±4.78
GCDCA	4.69±5.64
TCDCA	1.95±4.03
Total of secondary bile acids	5.58±7.91
DCA	0.89±1.19
GDCA	0.99±1.88
TDCA	0.19±0.46
LCA	0.067±0.112
GLCA	0.020±0.048
TLCA	0.003±0.013
UDCA	1.13±2.38
GUDCA	2.21±5.56
TUDCA	0.07±0.24

Data are presented as number of patients, mean ± standard deviation.
CA: cholic acid, GCA: glycocholic acid, TCA: taurocholic acid, CDCA: chenodeoxycholic acid, GCDCA: glycochenodeoxycholic acid, TCDCA: taurochenodeoxycholic acid, DCA: deoxycholic acid, GDCA: glycodeoxycholic acid, TDCA: taurodeoxycholic acid, LCA: lithocholic acid, GLCA: glycolithocholic acid, TLCA: taurolithocholic acid, UDCA: ursodeoxycholic acid, GUDCA: glycoursodeoxycholic acid, TUDCA: tauroursodeoxycholic acid.

Figure 1 Tamai et al

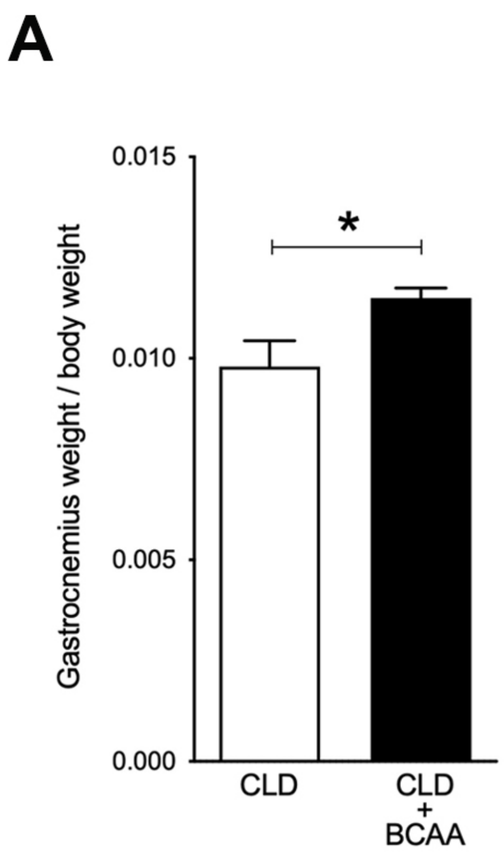

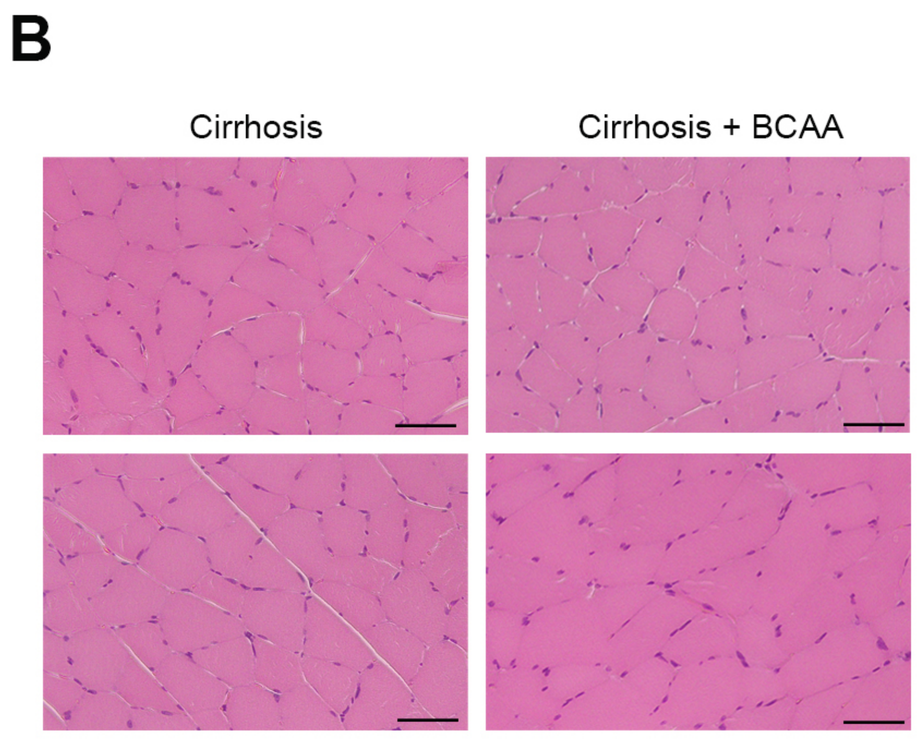

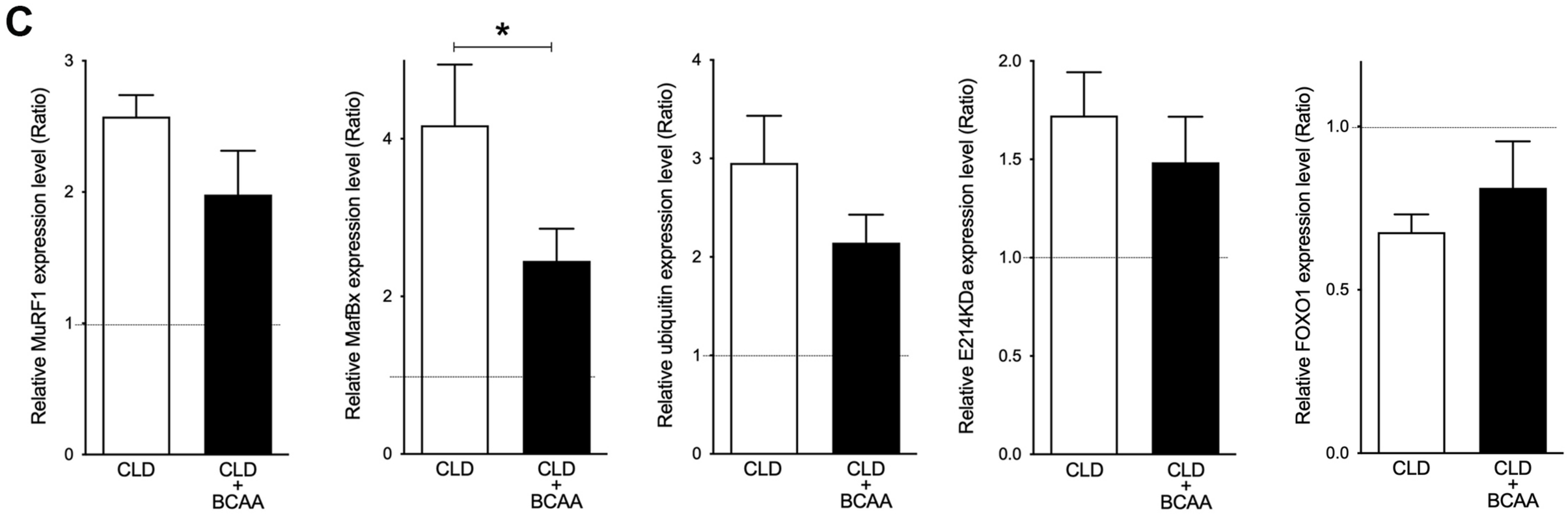

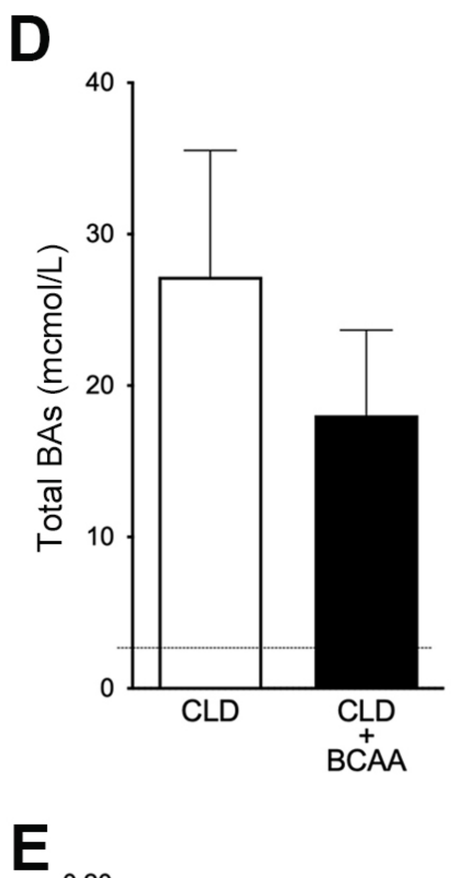

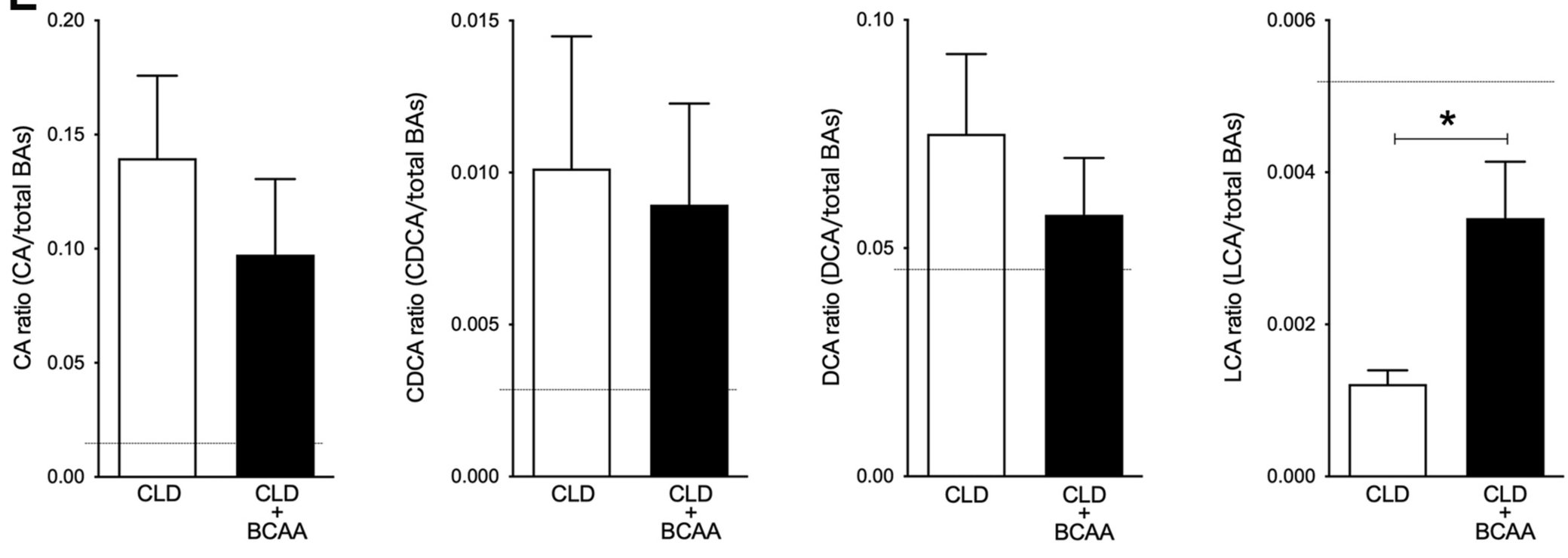

Figure 2 Tamai et al

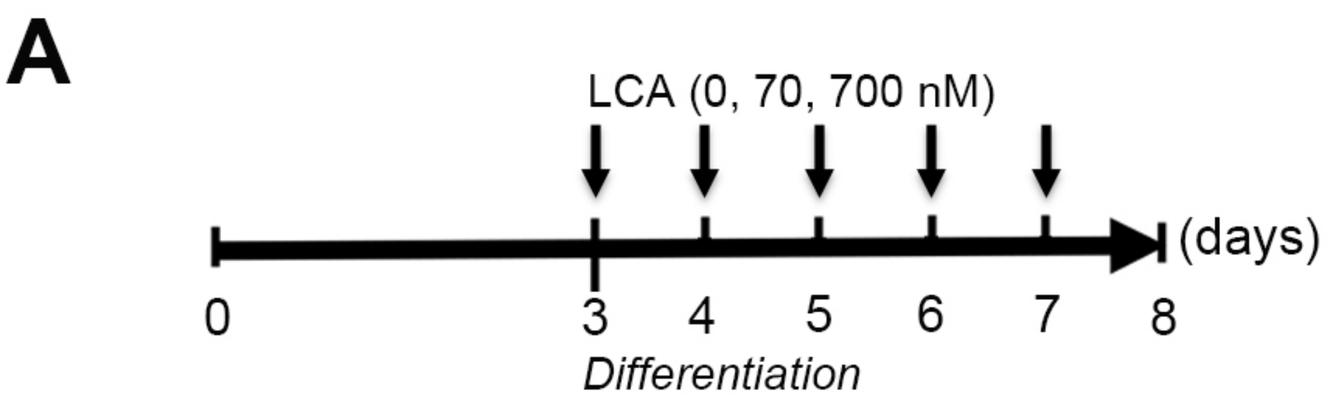

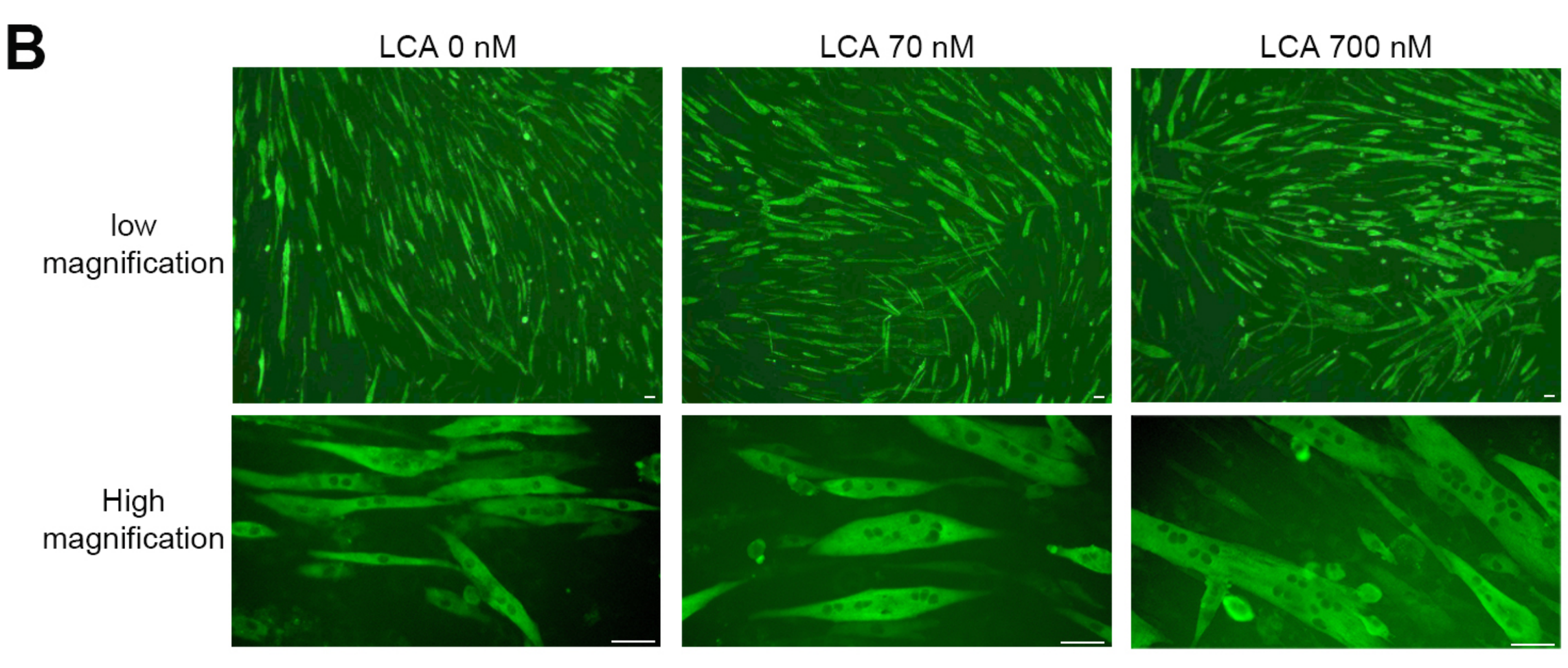

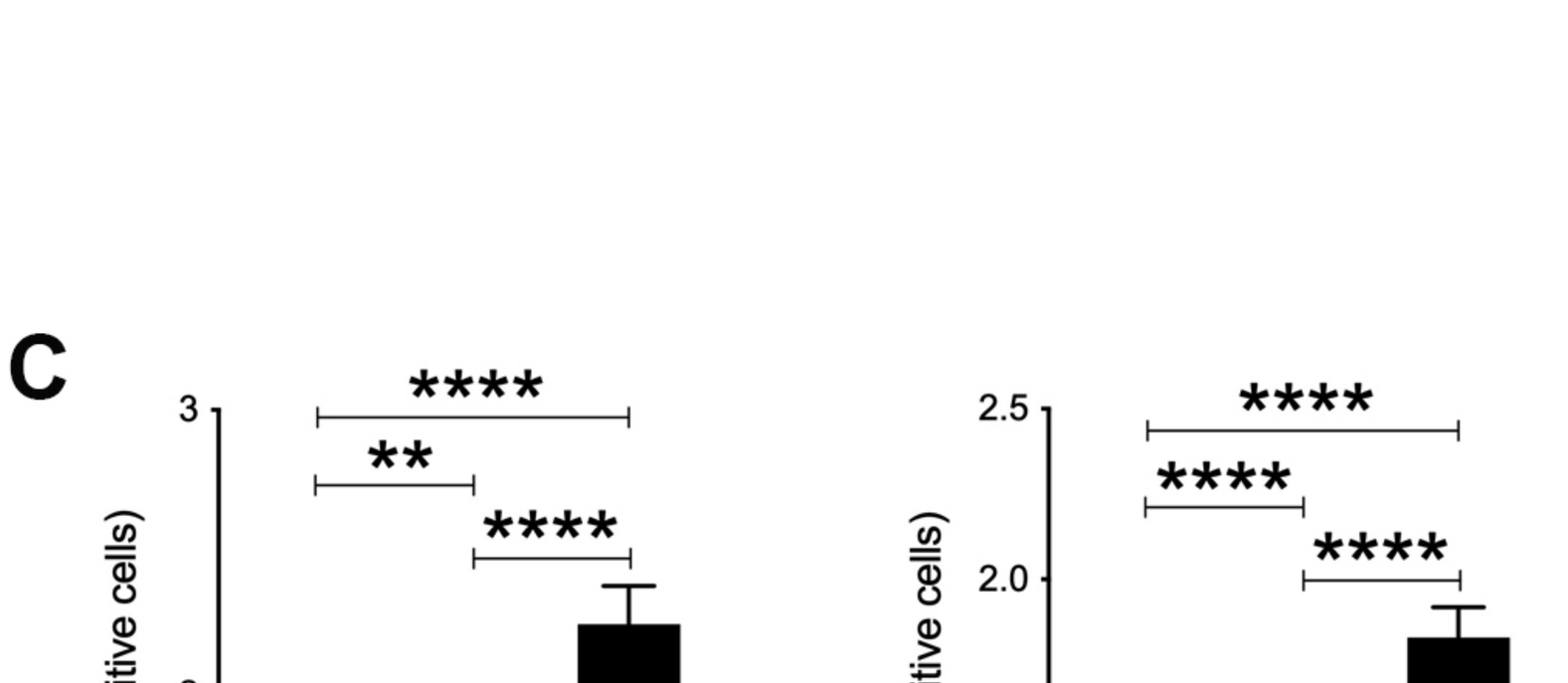

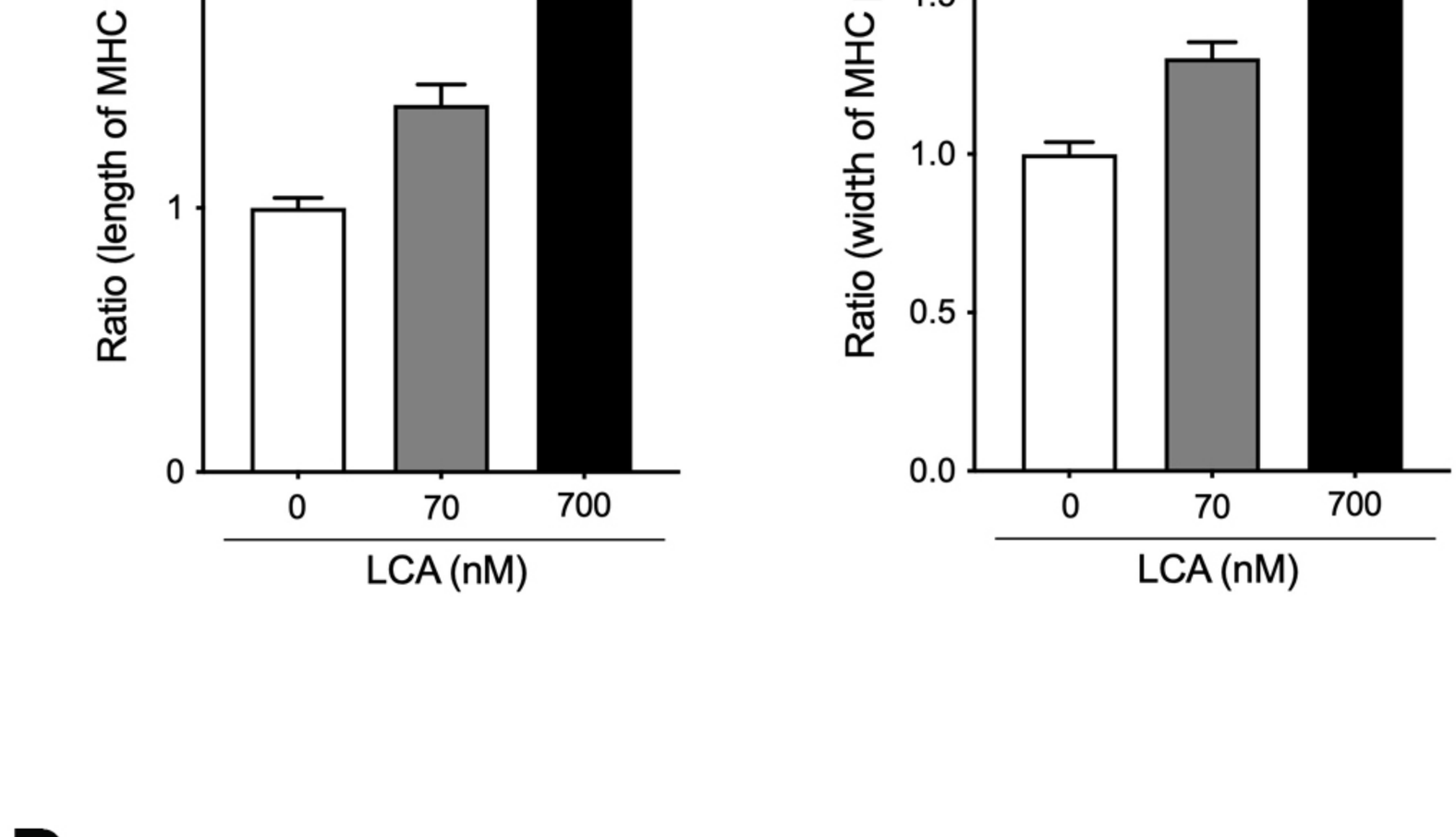

Figure 3 Tamai et al

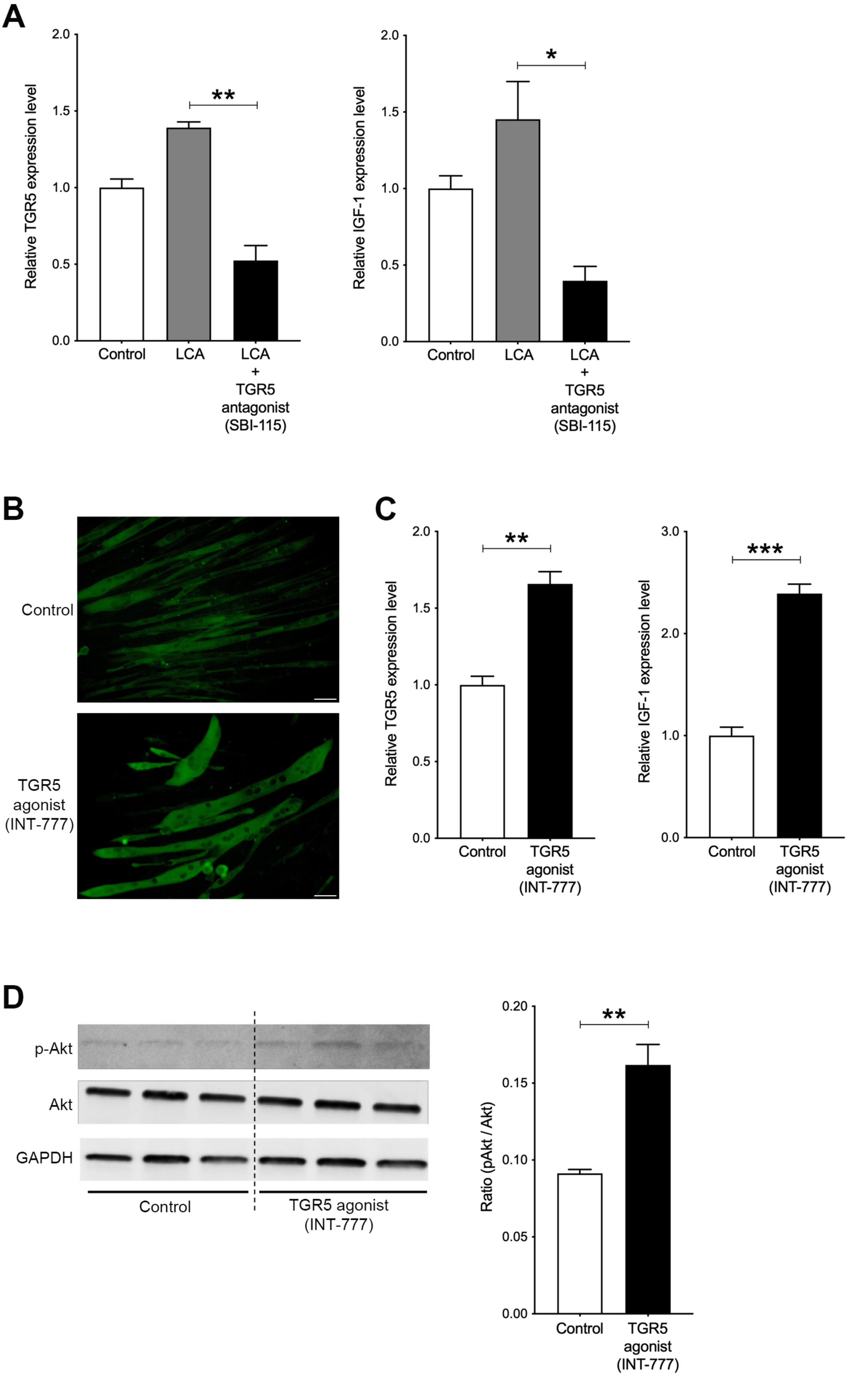

Figure 4 Tamai et al

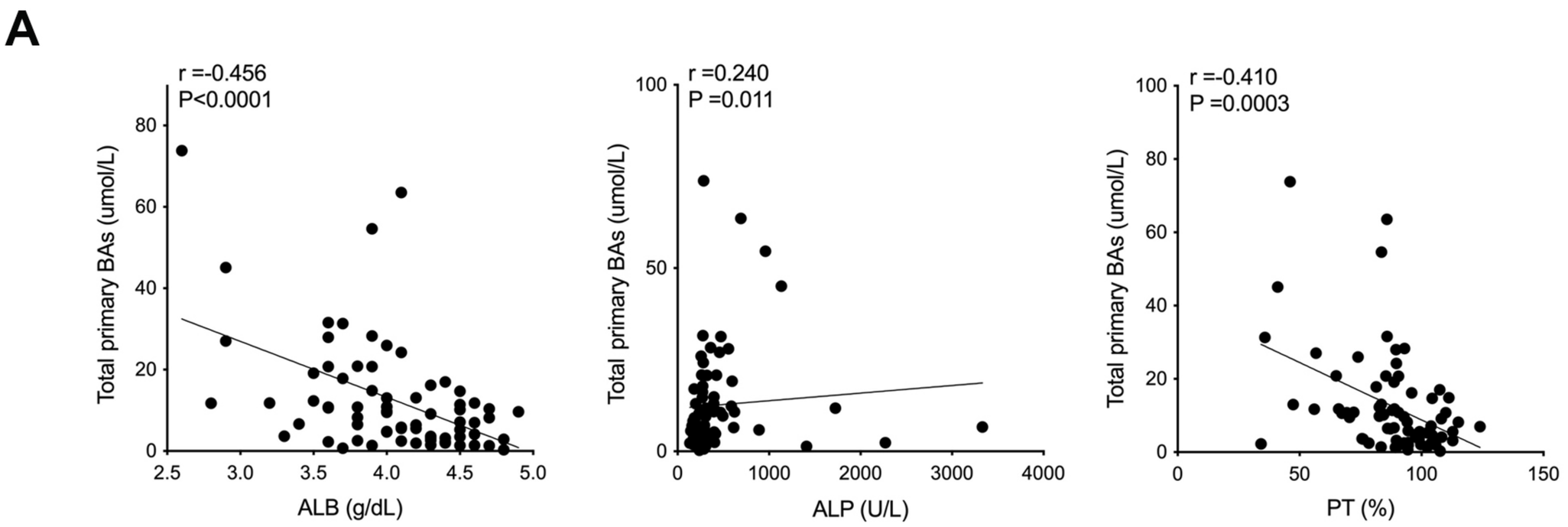

Figure 5 Tamai et al